Digital terrain mapping of the underside of sea ice from a small AUV

P. Wadhams, M. J. Doble

Digital terrain mapping of the underside of sea ice from a small AUV

P. Wadhams[1,2] and M. J. Doble[1,3]

Received 4 September 2007; accepted 23 November 2007; published 1 January 2008.

[1] In April 2007 the first three-dimensional digital terrain mapping of the underside of sea ice to be done from an ice-launched autonomous underwater vehicle (AUV) was carried out at an ice camp in the Beaufort Sea using the Gavia vehicle, which could be launched and recovered through 3 × 1 m holes. Gavia was equipped with a GeoSwath 500 kHz interferometric sonar system, which yielded swaths of typical width 80 m. The imagery showed the morphological distinctions between first-year (FY) and multi-year (MY) ice undersides, the contrast between the shapes of FY and MY ridges, and the appearance of refrozen leads. Ice drafts were validated by drilling, and it was found that ridge slope statistics and local probability density functions (PDFs) of draft could be derived with high precision. The special opportunities offered by access to 3-D mapping are pointed out. **Citation:** Wadhams, P., and M. J. Doble (2008), Digital terrain mapping of the underside of sea ice from a small AUV, *Geophys. Res. Lett.*, *35*, L01501, doi:10.1029/2007GL031921.

1. Introduction

[2] In recent years the autonomous underwater vehicle (AUV) has been developed as a method for obtaining data from under sea ice. AUVs are more readily available than military submarines and are more suitable for controlled small-scale surveys. The earliest AUV experiments under ice were carried out in the Beaufort Sea in 1972 using UARS (Unmanned Arctic Research Submersible) equipped with three narrow-beam upward sonars [*Francois and Nodland*, 1972; *Francois*, 1977]. *Bowen and Topham* [1996] mounted an upward-looking sonar on an ROV to build up a digital elevation map (DEM) of a Beaufort Sea first year ice ridge in April 1991. The vehicle was piloted along 32 tracks from two deployment holes, to cover an area of 150 × 300 m. The next under-ice use of an AUV was during the winter Lead Experiment (LeadEx) in 1992, in the Beaufort Sea [*Morison and McPhee*, 1998]. The 1.6 m long vehicle carried a CTD and was launched and recovered from a lead, homing to an acoustic beacon before recovery in a net. The Canadian Defence Research Establishment (Atlantic) used a large AUV for cable-laying in the Arctic in 1996 [*Ferguson et al.*, 1999]. *Hayes and Morison* [2002] used a REMUS-derived AUV to measure turbulent fluxes of heat, salt and momentum and ice draft profiles during the SHEBA project in 1997–8, while single-beam upward sonar data were collected in the Antarctic from the UK Autosub vehicle [*Brierley et al.*, 2002] in 2001.

[3] The first two-dimensional ice data were obtained in February 2002, when a Maridan Martin 150 AUV was used in the Greenland Sea [*Wadhams et al.*, 2004], equipped with a Tritech SeaKing 675 kHz sidescan sonar, a CTD and an ADCP. The sidescan sonar generated imagery of first- and multi-year ice floes in the marginal ice zone of the winter polar pack ice, while the upward channel generated a profile of ice draft.

[4] The next technical advance was the use of multibeam sonar from an AUV to obtain three-dimensional maps of the ice underside. This was achieved in August 2004 using Autosub off NE Greenland, equipped with a Kongsberg EM2000 sonar system [*Wadhams et al.*, 2006]. More than 450 track-km were obtained under first- and multi-year fast ice. The same vehicle later collected multibeam sonar data under the Fimbul ice shelf in the Antarctic [*Nicholls et al.*, 2006] before being lost there.

[5] The main disadvantage of large AUVs such as Autosub is that they must be deployed from a ship, as they are too long (6.7 m) and heavy (weight in air 3600 kg) for deployment through the ice. The ship must find an ice-free area of adequate size for launch and recovery, and must use a crane or gantry. This limits the use of the vehicle to open ice areas or, as with the 2004 experiment, to a location where close pack ice is found within a fixed ice edge, so that launch and recovery can be in open water while the vehicle transects are under the ice.

[6] For many applications it would be preferable to launch an AUV through a hole in the ice, to which it can return. This would enable the vehicle to be used to target a specific local ice regime of special interest. This aim was achieved successfully in April 2007 at the Applied Physics Laboratory ice station (APLIS) in the Beaufort Sea using the modular Gavia AUV manufactured by Hafmynd Ehf of Reykjavik, Iceland. We report here on the scientific results obtained.

2. Experiments

[7] The Gavia vehicle used at APLIS was 3.1 m long, weighed only 80 kg in air, and was thus capable of being manhandled. It was fitted with a GeoSwath 500 kHz interferometric sonar system built by GeoAcoustics Ltd. of Great Yarmouth, UK. The sonar is normally used to look downwards at the seafloor, but for under-ice operations the vehicle was ballasted to run inverted so that all instruments looked upwards at the ice underside. For navigation, the vehicle was equipped with a Kearfott IN-24 inertial navigation system (INS), coupled to a Doppler velocity log

[1]Department of Applied Mathematics and Theoretical Physics, University of Cambridge, Cambridge, U. K.
[2]Laboratoire d'Océanographie de Villefranche, Université Pierre et Marie Curie, Villefranche-sur-Mer, France.
[3]Temporarily at Laboratoire d'Océanographie de Villefranche, Université Pierre et Marie Curie, Villefranche-sur-Mer, France.

0094-8276/08/2007GL031921

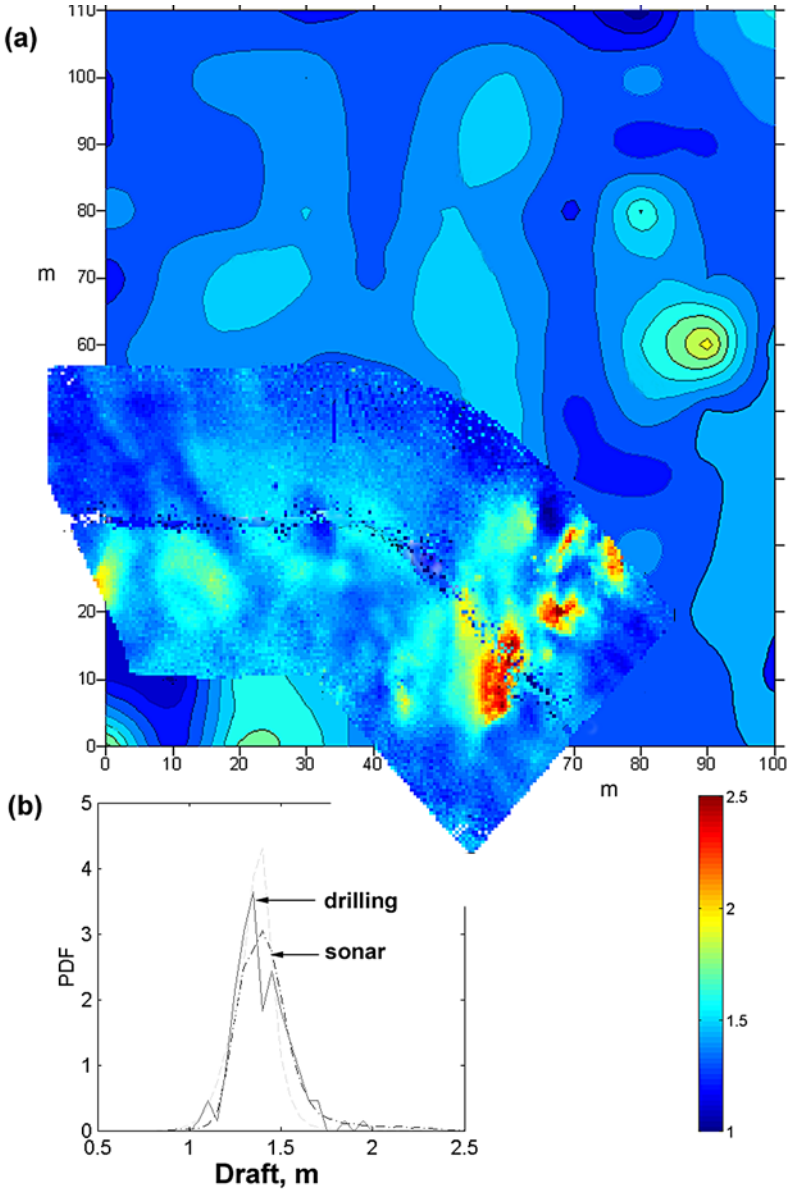

Figure 1. Contour map of drilling-derived ice draft (background image), compared to an overlapping sonar swath (foreground image). The color scale shows the drafts in metres. The deployment hole was near the center of the drilling site. The AUV ran at 10 m depth. Figure 1b shows PDFs of ice draft for two runs under site 1, plotted together with the PDF derived from the drilling. The PDFs have been shifted to maximise the cross-correlation between drilling- and sonar-derived data, giving an offset of minus 14 cm to the sonar data.

(DVL) which tracked its progress across the ice underside. Further technical details are given in a forthcoming publication.

[8] The experiments in April 2007 formed part of the Sedna project (www.research.iarc.uaf.edu/SEDNA/) led by University of Alaska, Fairbanks (UAF), a multi-sensor survey of the region around a camp which was originally established near 73°N, 145°W by the Arctic Submarine Laboratory, San Diego, as a base for acoustic experiments with US and British submarines. The AUV measurements thus benefited from multiple validation studies by other sensors including a submarine survey of the site carried out by the first author in March 2007 aboard HMS *Tireless*. AUV surveys were done jointly with laser profilometer (freeboard) and electromagnetic induction (thickness) overflights, and merged analyses will be reported in future publications.

[9] Two sites were used for the AUV experiments. The first was a region of first-year ice which did not contain well-defined ridges, but was mainly undeformed ice with some variability of thickness due to single blocks. The second site was close to a first-year ridge which was observed to have formed on April 2, eight days before our work began. In each case a 3 × 1 m hole was melted by a hot water drill, which allowed the AUV to be floated horizontally and made ballasting and mission preparation

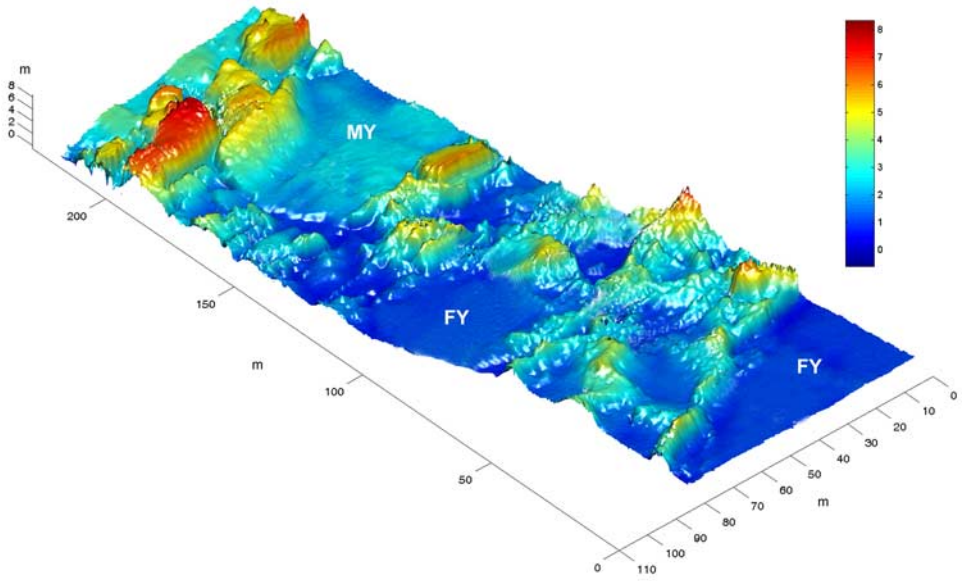

Figure 2. Sonar swath west of the deployment hole, plotted at 2× vertical exaggeration, showing (right-to-left), level FY ice, deformed FY ice, level MY ice and a MY ice ridge. The contrasting roughness of FY and MY deformed ice is clearly shown. The color scale shows the draft in meters. Running depth of the vehicle was 20 m. On this plot, as well as Figure 3 and Figure 4, sparse solutions at the zenith have been interpolated for visual effect, but are not included in statistical analyses.

easier. A heated canvas hut mounted on a sled was placed over the hole to provide shelter.

3. Results

3.1. First Site

[10] During the first experiments it was found that, in the absence of an acoustic homing system, the vehicle did not return perfectly to the small hole after a mission. It would typically return to within 10–20 m of the hole but then drift further away during its rise from running depth. Divers were available, but such recovery methods would have severely limited the number of missions per day. The decision was therefore taken to run the vehicle tethered to a 400 m kevlar line, fixed to an eye at mid-length on the vehicle so as to minimise the effect of line drag on the mission. This was found to work well, with little or no degradation of the vehicle's diving or turning performance, though it significantly limited the radius of operations.

[11] Seven runs were carried out at this site. Figure 1 inset shows a contour map of one section, with an apparent modal ice draft of about 1.4 m. The plot shows range/angle solutions binned into 0.5 × 0.5 m squares, with the value of each bin being a weighted mean of all the points within it. Typically about 20 points contribute to each bin. The centre-line of the curved section shows data dropouts directly above the vehicle. The nature of the GeoSwath instrument often results in poorly-resolved data at zenith if the target is relatively flat, since the system samples a range series of angles and the target is all at the same range at zenith. If the target directly above the vehicle has significant relief, however, it will be well-sampled. Empty bins are also evident during the turn, due to the very tightly-constrained beam width along-track (0.5°). Overall data density is extremely high, however – the short section displayed comprises over 360,000 data points – giving reliable spatial statistics from a relatively small area. A full description of GeoSwath system performance is give by *Hiller and Hogarth* [2005].

[12] The sonar data were ground-truthed by drilling at 10 m intervals over a 100 × 110 m area centred on the hole. Figure 1 shows the resulting contour plot of ice draft - interpolated using the Kriging method – with the sonar run which crosses its SW corner superimposed on it. PDFs of drilled and sonar-derived drafts are shown overlaid in Figure 1b. The two curves are the same shape and were shifted to maximise the cross-correlation, giving an offset of −14 cm. This is in agreement with the physical separation of sensors within the vehicle and allows the sonar results to be referenced to zero draft. It is also clear from visual inspection of Figure 1 and its inset that the sonar run generates a higher resolution picture of the ice cover morphology than the 132 holes which required two days to drill. Sound velocity was calculated using temperature and salinity data from casts with a Seabird SBE-19 CTD, and verified with Gavia's on board sound velocimeter.

3.2. Second Site

[13] The second site was close to a pressure ridge in first-year ice. Multi-year ice lay within range of the AUV to the west and a thin (48 cm draft) refrozen lead lay on the far side of the ridge (east). The experimental strategy was to send out the AUV along a track to a distance of 100–300 m from the hole, make a wide turn and return to the hole. The return run was usually deeper than the outward leg, to ensure that the tether line was pulled down, away from any obstructions. The line was also slightly negatively buoyant.

[14] Figure 2 is an example of the data obtained, from a 300 m run west of the ice hole. Several ice types are shown in some detail. The vehicle first encounters relatively

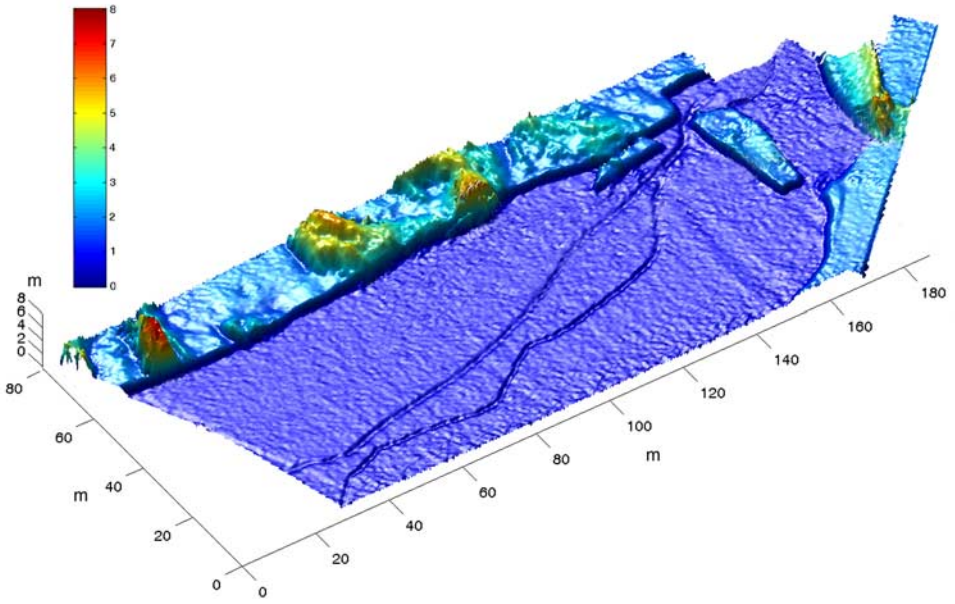

Figure 3. A refrozen lead, plotted with 2× vertical exaggeration, showing the level of detail available from the GeoSwath system. The lead displays two narrow cracks and is bordered by FY ice with fragments of ridges/rubble. The 'dappled' texture of the refrozen lead results from the ±3 cm standard error of each 0.5 × 0.5 m bin; the lead is smoother in reality. The cross-track 'trough' near the right hand end of the run is a roll artefact caused by a navigational dropout. Vehicle depth was 20 m.

smooth FY ice with a modal draft of 1.6 m (estimated thickness 1.78 m), then a complex rubble field composed of the same ice. Further along track a thicker multi-year floe (modal draft 2.9 m) is encountered, with an 8.8 m draft multi-year ridge embedded within it. The contrast between the old, rounded, ice blocks of the multi-year ridge and the rougher, first-year, deformed ice is particularly striking, and can be compared with a first-year/multi-year ridge juxtaposition in figure 3d of *Wadhams et al.* [2006].

[15] Figure 3 shows how the system images a thin (modal draft 0.48 m) refrozen lead. The lead exhibits two meandering cracks, which have refrozen to a draft of only 0.2 m across their 0.5 m width. The figure shows the sharp boundary between the lead and deformed FY ice (modal draft 1.6 m), with displaced pieces of FY ice embedded in the refrozen lead matrix. When sidescan sonar imagery of sea ice first became available [*Wadhams*, 1988], it was seen that the underside of FY is morphologically quite different from that of MY ice. MY ice has an undulating surface with crater-like depressions (derived from the thermodynamic effects of top surface melt) while the FY underside is smooth but criss-crossed by cracks, many of which do not penetrate through to the upper surface. These are likely to be the start points for ridging when compressive stresses occur. The full 3-D mapping of the AUV not only shows these cracks but gives their depth and width.

[16] Figure 4 shows a section of the main study ridge, up to 16.80 m deep, from a run paralleling this feature. First-year ice forms most of the level area (modal draft 1.6 m), with an associated rubble area (modal draft 2.4 m) towards the bottom left of the plot and another thin ice area to the top right (modal draft 0.85 m). Observations by divers suggest that the extremely jagged topography indicated by the sonar, for instance in the ridge crest region (arrowed), is real and not an artefact.

[17] The study ridge can be compared with existing literature studies by estimating an equivalent slope angle for the ridge. We focus on the central parallel section of Figure 4 (between cuts at A and B) and determine the quantities V (volume of ice protruding from level ice horizon within deformed zone), L (length along ridge crest) and W (mean width of deformed zone), from which we derive

$$\tan\theta = 4V/LW^2 \quad (1)$$

where θ is the equivalent slope of a triangular ridge built on the same base, equal to 24.8° here. The largest statistical study of ridge slopes was by *Davis and Wadhams* [1995], who found in a sample of 729 ridges (both FY and MY) a modal slope of 18°, indicating that this recently-formed ridge has a relatively high steepness.

[18] Histograms for the sonar swaths are shown in Figure 5. Data from submarine sonar profiles of the ice underside [e.g., *Wadhams*, 2000], analysed in 50 km sections, usually show a PDF which has one or more peaks for the preferred drafts of undeformed ice, followed by a tail which takes the form of a negative exponential, describing the statistical sum of all the ridged ice present. The present data are drawn from a small area of icefield containing only one or two major ridge features, but also demonstrate this relationship, as suggested by the inset to Figure 5 drawn on a linear-log scale. The slope of the negative exponential is a measure of the state of deformation of the icefield and the relative contributions of shallow and deep ridges to the ice regime.

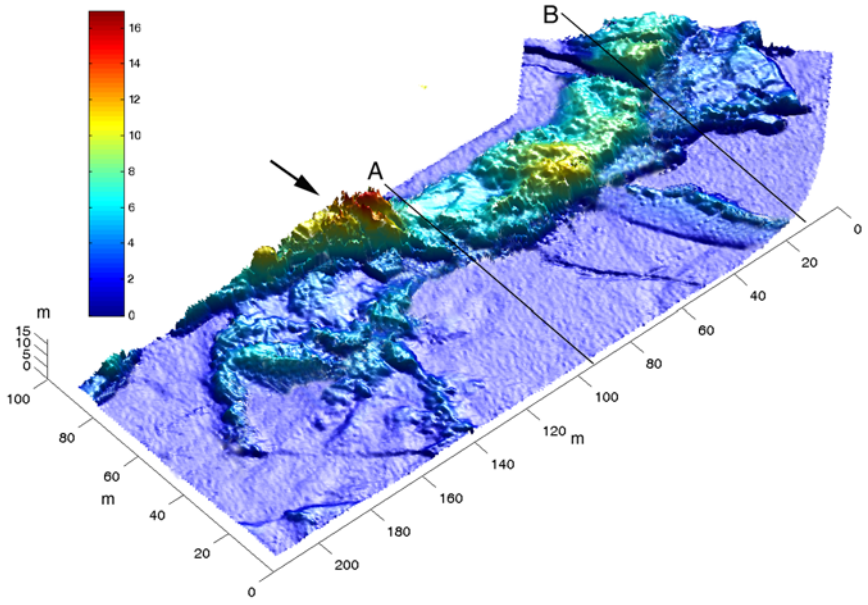

Figure 4. The main study ridge. The plot is displayed without vertical exaggeration, and shows the very steep topography of this young ridge. Maximum draft in the swath is 16.8 m, and the AUV was running at 25 m depth. The dappled character of the FY ice evident in this backlit image arises from the ±3 cm standard error in individual bins.

The inset suggests that the best fit to the slope parameter b in the negative exponential

$$P = A \exp(-b\,h) \tag{2}$$

where P is probability density, h is ice draft, is b = 0.46. Comparison with other sets of PDFs, for instance a set of runs in the Trans Polar Drift Stream [*Wadhams*, 1992], shows that the slope is slightly greater than ice within the Arctic Basin (b = 0.34 at 82°N) but much less than melting ice in the East Greenland Current south of 79°N (b in the region of 0.9). The slope value is identical with datasets drawn from the Arctic Basin north of Ellesmere Island and Greenland [*Wadhams*, 1992, Figure 6]. This admittedly small slice of an Arctic ice regime is therefore rather typical of the Arctic Basin in its roughness criteria.

4. Conclusions

[19] The unique contribution to Arctic ice research offered by the Gavia/GeoSwath AUV-sensor combination stems from two attributes: its size, and the type of imagery obtained.

[20] The use of an AUV that is small enough to be manhandled gives a powerful boost to under-ice research, as it can be used in almost any field context – from ice camps, offshore structures, ships or aircraft touchdowns. All that is needed is the ability to make a suitable hole, a source of power for recharging batteries (e.g. a petrol generator), and, if possible, a tent or hut to cover the hole. One can then deploy the vehicle near a feature of special interest and survey its three-dimensional underside topography with high precision. A continuing problem is that the full advantage of an AUV, its autonomy, can only be realised if it is untethered, and this requires either a significant advance in navigational accuracy or the implementation of acoustic homing. The use of smaller holes would also aid flexibility; Gavia has the ability to be launched vertically through a small diameter hole which can be drilled quickly by conventional techniques, but this would make setup and recovery more awkward.

[21] The advent of full 3-dimensional mapping, first attained in 2004 [*Wadhams et al.*, 2006] and now amplified by the flexible Gavia/GeoSwath system, literally provides a new dimension to ice morphology studies, permitting new types of statistic to be generated. Preferred thicknesses of undeformed first- and multi-year ice can be determined with precision, and the shapes of PDFs determined for small areas of icefield, although the correlation length of about

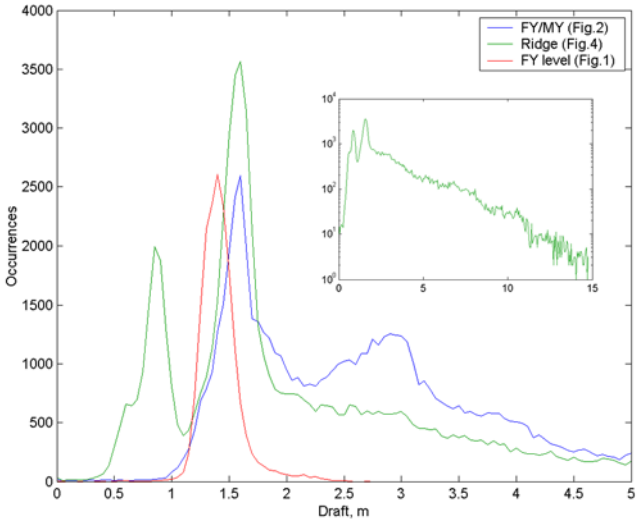

Figure 5. Ice draft occurrences for the various swaths displayed in previous figures. Inset shows data from Figure 4 drawn on a linear-log scale to show the negative exponential tail.

100 m for Arctic sea ice means that the generation of large-scale PDFs is only slightly more efficient than using a narrow beam sonar (since only two independent parallel profiles can be obtained from a single swath). Much more important are the completely new 3-D statistics of autocorrelation, spectra, fractals and connectivity properties of the ice underside that are now possible, with implications for studies of turbulence, sonar backscatter and oil containment among many other applications.

[22] It is important to continue to develop optimum AUV-sonar combinations such as this for the serious task of mapping the changing ice cover, in particular to follow the changes in topography and under-ice structure which accompany the thinning currently being experienced by Arctic sea ice. Deployment of this sensor combination to study the very different under-ice topography of the Antarctic would also be most fruitful.

[23] **Acknowledgments.** This work was supported by the National Science Foundation Office of Polar Programs under grant OPP0612527 to University of Alaska Fairbanks. Additional support was provided by the DAMOCLES project, grant no. 018509 of the European Union 6th Framework Program. We are indebted to Richard Yeo and Eggert Magnusson of Hafmynd for technical support and especially to Jeremy Wilkinson (Scottish Association for Marine Science, Oban, Scotland) for field support and collaboration in AUV development. We also thank all at the Applied Physics Laboratory Ice Station for their help during the camp, especially Jenny Hutchings (UAF) for the invitation to take part in the Sedna experiment.

References

Bowen, R. G., and D. R. Topham (1996), A study of the morphology of a discontinuous section of a first year Arctic pressure ridge, *Cold Reg. Sci. Technol.*, *24*, 83–100.

Brierley, A. S., N. W. Millard, S. D. McPhail, P. Stevenson, M. Pebody, J. Perrett, M. Squires, and G. Griffiths (2002), Antarctic krill under sea ice: Elevated abundance in a narrow band just south of ice edge, *Science*, *295*, 1890–1892.

Davis, N. R., and P. Wadhams (1995), A statistical analysis of Arctic pressure ridge morphology, *J. Geophys. Res.*, *100*, 10,915–10,925.

Ferguson, J., A. Pope, B. Butler, and R. Verrall (1999), Theseus AUV: Two record-breaking missions, *Sea Technol.*, *40*, 65–70.

Francois, R. E. (1977), High resolution observations of under-ice morphology, *Tech. Rep. APL-UW 7712*, 30 pp., Appl. Phys. Lab., Univ. of Wash., Seattle.

Francois, R. E. and W. K. Nodland (1972), Unmanned Arctic Research Submersible (UARS) system development and test report, *Tech. Rep., APL-UW 7219*, 88 pp., Appl. Phys. Lab., Univ. of Wash., Seattle.

Hayes, D. R., and J. H. Morison (2002), Determining turbulent vertical velocity and fluxes of heat and salt with an autonomous underwater vehicle, *J. Atmos. Oceanic Technol.*, *19*, 759–779.

Hiller, T. M., and P. Hogarth (2005), The use of phase measuring (interferometric) sonars: Choosing appropriate data processing methodologies, *Int. Hydrogr. Rev.*, *6*, 1–12.

Morison, J. H., and M. G. McPhee (1998), Lead convection measured with an autonomous underwater vehicle, *J. Geophys. Res.*, *103*, 3257–3281.

Nicholls, K. W., et al. (2006), Measurements beneath an Antarctic ice shelf using an autonomous underwater vehicle, *Geophys. Res. Lett.*, *33*, L08612, doi:10.1029/2006GL025998.

Wadhams, P. (1988), The underside of Arctic sea ice imaged by sidescan sonar, *Nature*, *333*, 161–164.

Wadhams, P. (1992), Sea ice thickness distribution in the Greenland Sea and Eurasian Basin, May 1987, *J. Geophys. Res.*, *97*, 5331–5348.

Wadhams, P. (2000), *Ice in the Ocean*, 368 pp., Taylor and Francis, Philadelphia, Pa.

Wadhams, P., J. P. Wilkinson, and A. Kaletzky (2004), Sidescan sonar imagery of the winter marginal ice zone obtained from an AUV, *J. Atmos. Oceanic Technol.*, *21*, 1462–1470.

Wadhams, P., J. P. Wilkinson, and S. D. McPhail (2006), A new view of the underside of Arctic sea ice, *Geophys. Res. Lett.*, *33*, L04501, doi:10.1029/2005GL025131.

M. J. Doble and P. Wadhams, Department of Applied Mathematics and Theoretical Physics, University of Cambridge, Cambridge CB3 0WB, UK. (pw11@damtp.cam.ac.uk)